Prediction of new T_{cc} states of D^*D^* and $D_s^*D^*$ molecular nature

L. R. Dai,[1,2,*] R. Molina,[2,†] and E. Oset[2,‡]

[1]*School of Science, Huzhou University, Huzhou, 313000 Zhejiang, China*
[2]*Departamento de Física Teórica and IFIC, Centro Mixto Universidad de Valencia-CSIC Institutos de Investigación de Paterna, Aptdo.22085, 46071 Valencia, Spain*

(Received 5 November 2021; accepted 19 January 2022; published 31 January 2022)

We extend the theoretical framework used to describe the T_{cc} state as a molecular state of D^*D and make predictions for the D^*D^* and $D_s^*D^*$ systems, finding that they lead to bound states only in the $J^P = 1^+$ channel. Using input needed to describe the T_{cc} state, basically one parameter to regularize the loops of the Bethe-Salpeter equation, we find bound states with bindings of the order of MeV and similar widths for the D^*D^* system, while the $D_s^*D^*$ system develops a strong cusp around the threshold.

DOI: 10.1103/PhysRevD.105.016029

I. INTRODUCTION

The discovery of the mesonic T_{cc} state with two open charm quarks [1–4] has brought a new example of an exotic meson state, challenging the standard nature of mesons as $q\bar{q}$ states. The reaction of the theory community has been fast and many articles have been written proposing different interpretations about the nature of the state [5–27]. Rates in production reactions had been calculated prior to the T_{cc} discovery [28]. The relevant analysis carried out in [29] by means of a unitary amplitude, with explicit consideration of the experimental resolution, has shown that the width of the T_{cc} state is much smaller than the one extracted from the raw data in [4], and in line with the width obtained in [8]. Similar conclusions are obtained in [30]. The proximity of the peak position in [29] to the D^*D threshold strongly supports the D^*D nature of this state, something assumed in most of the works done on the T_{cc} state. In [8] the state was studied within a unitary coupled channel approach with the $D^{*+}D^0$ and $D^{*0}D^+$ channels and the interaction was obtained from the exchange of vector mesons in a straight extrapolation of the local hidden gauge approach [31–34] to the charm sector [35]. The only parameter in [8] was a regulator in the meson meson loop function of the Bethe-Salpeter equation, which was tuned to obtain the mass of the state at the right position, then the width and the $D^0D^0\pi^+$ mass distribution were obtained in good agreement with experiments, with a width of around 43 KeV.

Given the fact that heavy quark spin symmetry [36–38] allows us to relate the D and D^* sectors, it is tempting to extend the results of [8] to the D^*D^* system to make predictions on this state. The task is rendered easier because this system and the $D_s^*D^*$ were studied before the recent experimental finding on the D^*D system [4] in [39]. Indeed, in [39] it was found that the D^*D^* system in isospin $I = 0$, and $J^P = 1^+$ and the $D_s^*D^*$ system in $I = 1/2, J^P = 1^+$ had an attractive potential, strong enough to support a bound state, and predictions were done with a binding of around 35 MeV. The D^*D^* with $I = 1$ and $D_s^*D_s^*$ systems were also investigated in [39] and the interaction was found repulsive, so we do not study these systems here.

The predictions for the binding are tied to the regulator of the meson meson loop function, and right now we have experimental information from [4,29] to fix it, such that more accurate predictions can be done. On the other hand, in [39] the width of the states was obtained from the pseudoscalar-pseudoscalar decay channel, which in the present case is forbidden by spin-parity conservation. Yet, there is another source of decay which is the pseudoscalar-vector channel, which we will evaluate here. This decay channel was investigated in the study of the $D^*\bar{K}^*$ system [40] which produced a bound state in [39] and was shown in [40] to be suited to reproduce the properties of the $X_0(2866)$ state recently observed by the LHCb Collaboration in [41].

The width of the T_{cc} state is tied to the $D^* \to \pi D$ decay [29], and results in about 40 KeV–50 KeV. On the contrary, here the D^*D^* and $D_s^*D^*$ systems will decay into a pseudoscalar-vector system which has a much larger phase space for decay than the $D^* \to \pi D$. Hence, we can already guess that we shall have a much larger width, yet, still reasonably small, as one can induce from the results of [40].

*dailianrong@zjhu.edu.cn
†Raquel.Molina@ific.uv.es
‡oset@ific.uv.es

The D^*D^* system has been relatively unexplored from the molecular point of view. It is studied in [42] using meson exchange for the interaction and in [43] using the exchange of vector mesons guided by the local hidden gauge approach. Only the diagonal-interaction and no decay channels are considered in [43], which aims at providing guidelines on possible states at the qualitative level. The D^*D^* system in $I=0$ and $J^P=1^+$ appears in [43] as a candidate for a bound state, and in [30,44] it also appears as a bound state using arguments of heavy quark spin symmetry and the data of [4]. In [42] a state of $D^{(*)}D^{(*)}$ nature, without distinguishing between D^*D and D^*D^*, is also found to be a good candidate for a bound state in $I=0$ and $J^P=1^+$. Similarly, a possible $(D^{(*)}D^{(*)})_s$ state in $J^P=1^+$ is also reported in [42]. The widths are not considered in this latter work.

On the other hand there are many works dealing with mesons with two heavy quarks as tetraquark states, using quark models, sum rules or lattice QCD. The $QQq\bar{q}$ systems were studied already in [45] indicating an increased attraction on some channels as the ratio of M/m (heavy to light quark masses) increases, something corroborated in [46–48]. Calculations of binding energies of doubly heavy tetraquarks were done in [49–51] using different quark models, in [52–61] using QCD sum rules, lattice QCD calculation [62–70], and other models [71–73]. The predictions of the different models ranged from about 250 MeV above to 250 MeV below the meson-meson threshold, indicating the difficulties to make accurate predictions with these methods.

In the present work, with the background from the molecular studies discussed above and the valuable information from the T_{cc} state, we retake the task of studying the D^*D^* and $D_s^*D^*$ systems, paying attention to the decay channels, with the purpose of making a precise determination of the mass and widths of the bound states emerging from the interaction of these systems.

II. FORMALISM

A. Direct interaction

The interaction of D^*D^* and $D_s^*D^*$ is studied in [39]. It is based on the extrapolation of the local hidden-gauge approach [31–34] to the charm sector. The local hidden-gauge approach was first used in [74,75] to study the interaction between vector mesons in the $SU(3)$ sector. It contains a contact term and the exchange of vector mesons which requires a three-vector vertex. In [74,75] this interaction was shown to produce bound states or resonances which could be associated to existing states. Extrapolated to the charm sector, it predicted the pentaquark states with hidden charm and hidden charm and strangeness [35,76] which were found later by the LHCb Collaboration [77–79].

The basic ingredients to calculate the potential between two vectors are the Lagrangians

$$\mathcal{L}^{(c)} = \frac{g^2}{2}\langle V_\mu V_\nu V^\mu V^\nu - V_\nu V_\mu V^\mu V^\nu \rangle, \tag{1}$$

with $g = \frac{M_V}{2f}$ ($M_V = 800$ MeV, $f = 93$ MeV), and V_μ the $q\bar{q}$ matrix written in terms of vector mesons

$$V_\mu = \begin{pmatrix} \frac{\omega}{\sqrt{2}} + \frac{\rho^0}{\sqrt{2}} & \rho^+ & K^{*+} & \bar{D}^{*0} \\ \rho^- & \frac{\omega}{\sqrt{2}} - \frac{\rho^0}{\sqrt{2}} & K^{*0} & D^{*-} \\ K^{*-} & \bar{K}^{*0} & \phi & D_s^{*-} \\ D^{*0} & D^{*+} & D_s^{*+} & J/\psi \end{pmatrix}_\mu , \tag{2}$$

and

$$\mathcal{L}_{VVV} = ig\langle (V^\mu \partial_\nu V_\mu - \partial_\nu V_\mu V^\mu) V^\nu \rangle. \tag{3}$$

$\mathcal{L}^{(c)}$ is a contact term and $\mathcal{L}_{VVV}$ stands for the three-vector vertex. By means of it, one generates an interaction between vectors exchanging vector mesons. The mechanisms for the interaction are depicted in Fig. 1.

In Table XVI of [39] it was shown that the contact term for D^*D^* in $I=0$ gives no contribution. By contrast, the vector exchange term gives null contribution for spin $J=0$, 2 but produces an attractive potential in $J^P=1^+$,

$$\begin{aligned} V_{D^*D^*\to D^*D^*} = & \frac{1}{4} g^2 \left(\frac{2}{m_{J/\psi}^2} + \frac{1}{m_\omega^2} - \frac{3}{m_\rho^2} \right) \\ & \times \{ (p_1+p_4)\cdot(p_2+p_3) \\ & + (p_1+p_3)\cdot(p_2+p_4) \}. \end{aligned} \tag{4}$$

In Table XVII of [39] it is shown that for $I=1$ the interaction for $J=0$, 2 is repulsive and null for $J=1$. The situation is similar for the $D_s^*D_s^*$ system, which has $I=0$, with repulsive interaction in $J=0$, 2 and null interaction for $J=1$ (see Table XIX of [39]). On the contrary, as shown in Table XVIII of [39], the $D_s^*D^*$ system, which has $I=\frac{1}{2}$, gives attraction for $J=1$ and repulsion for $J=0$, 2.

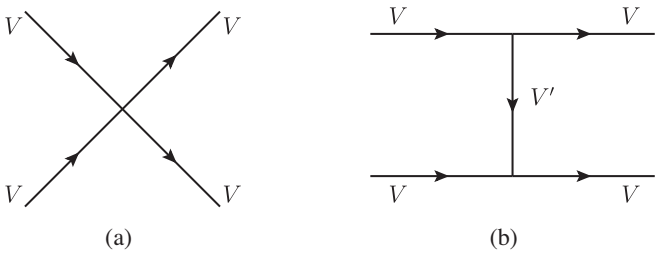

FIG. 1. Terms for the VV interaction: (a) contact term, (b) vector exchange.

We are thus left with two candidates for bound states D^*D^* with $I=0, J^P=1^+$ and $D_s^*D^*$ with $I=\frac{1}{2}, J^P=1^+$. The interaction for this latter case is given by

$$V_{D_s^*D^*\to D_s^*D^*} = -\frac{g^2(p_1+p_4)\cdot(p_2+p_3)}{m_{K^*}^2} + \frac{g^2(p_1+p_3)\cdot(p_2+p_4)}{m_{J/\psi^2}}. \quad (5)$$

Note that $(p_1+p_3)\cdot(p_2+p_4)$ projected in s-wave can be written as [80]

$$\frac{1}{2}\{3s-(M_1^2+M_2^2+M_3^2+M_4^2)-\frac{1}{s}(M_1^2-M_2^2)(M_3^2-M_4^2)\}. \quad (6)$$

In [39] the T-matrix was obtained from these potentials using the Bethe-Salpeter equation

$$T=[1-VG]^{-1}V, \quad (7)$$

with G the intermediate vector-vector (VV) loop function which was regularized by means of a cutoff and also dimensional regularization. On the other hand, the pseudoscalar-pseudoscalar (PP) decay channels were considered for all the states studied there, but the VV states with 1^+ cannot decay to PP if we want to conserve spin and parity. Here we consider instead the decay into vector-pseudoscalar (VP) channels which will give a width to the bound states that we find.

B. Vector-pseudoscalar decay channels

1. $D^*D^* \to D^*D$ decay

We take the $I=0$ D^*D^* state. With the isospin doublets $(D^+, -D^0)$ and $(D^{*+}, -D^{*0})$, the $I=0$ state is given by

$$|D^*D^*, I=0\rangle = -\frac{1}{\sqrt{2}}|D^{*+}D^{*0}-D^{*0}D^{*+}\rangle. \quad (8)$$

This system can decay into $D^{*+}D^0$ or $D^{*0}D^+$ and we shall take into account these decays by means of the imaginary part of the box diagrams of Fig. 2. The diagrams shown in Fig. 2 have all the same structure and only the isospin coefficients are different. Note that intermediate D_s or D_s^* states are not possible while having two open charm quarks in the two-meson system. Taking the first diagram as reference and the coupling of π^0 to $D^{*+}D^{*+}$ as 1, by means of Clebsch-Gordan coefficients we find the weight

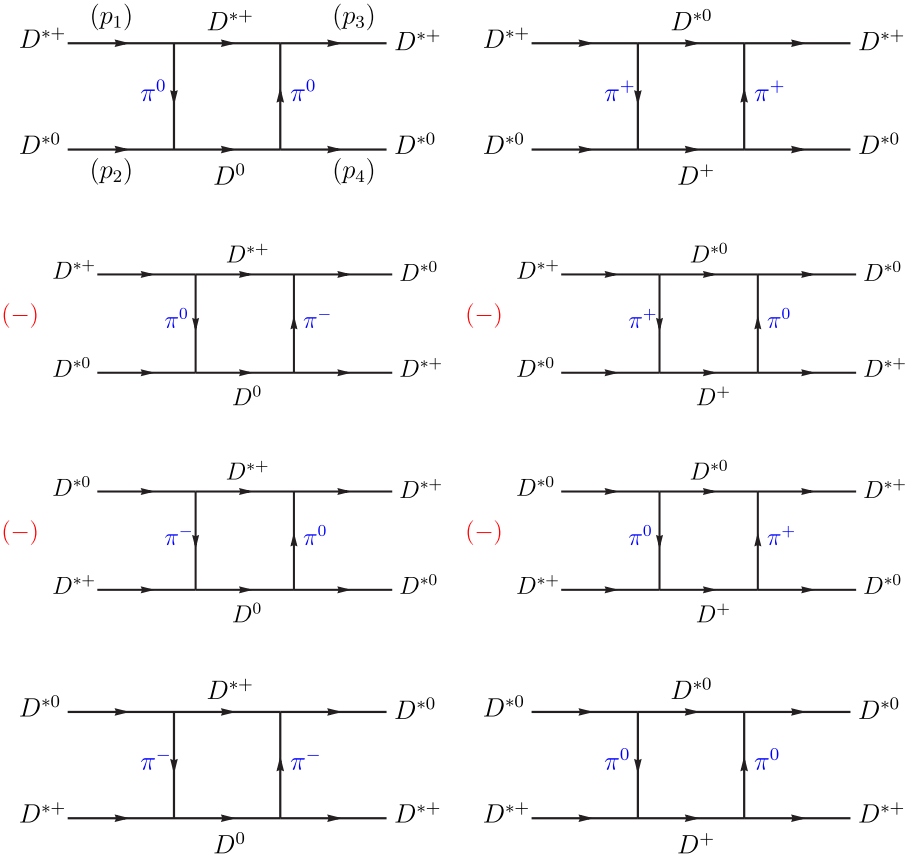

FIG. 2. Box diagrams according for $D^*D^*, I=0$ decay into $D^{*+}D^0$ and $D^{*0}D^+$.

-1 for $\pi^0 D^{*0} D^{*0}$, and $\sqrt{2}$ for π^+ or π^- coupling to $D^{*+} D^{*0}$ (consistent with our phase convention $\pi^+ = -|11\rangle$). The total weight of the diagrams is

$$\frac{1}{4}(1+2+2+4+4+2+2+1) = \frac{18}{4} = \frac{9}{2}.$$

We have to consider in addition the diagrams where the pseudoscalar meson is on the upper line of the diagram and the vector in the lower line, which are depicted in Fig. 3. If we take the second diagram of Fig. 3 as reference (with the exchange of two π^0), the rest of them are included as before and altogether we have a weight $\frac{9}{2}$ of the second diagram of Fig. 3. The set of diagrams must be completed exchanging the vectors $D^*(p_3) \leftrightarrow D^*(p_4)$ in the final state, given the identity of the two D^* in the final state (in the isospin formalism). Then the diagrams of Fig. 2 give rise to the diagrams of Fig. 4. We observe now that the third diagram of Fig. 4 (the one with two π^0 exchange) is equivalent to the first diagram of Fig. 2, except that $p_3, \boldsymbol{\epsilon}_3 \leftrightarrow p_4, \boldsymbol{\epsilon}_4$ ($\boldsymbol{\epsilon}_i$ is the polarization vector of particle i) are exchanged and there is a relative (-1) sign. The same happens when we exchange the final states of Fig. 3, which we do not depict. Altogether, the sum of the 32 diagrams can be calculated as shown in Fig. 5.

The evaluation of these diagrams requires now the use of two new vertices, the ordinary VPP coupling and the anomalous VVP coupling given by the Lagrangians

$$\mathcal{L}_{VPP} = -ig\langle [P, \partial_\mu P] V^\mu \rangle, \tag{9}$$

$$\mathcal{L}_{VVP} = \frac{G'}{\sqrt{2}} \epsilon^{\mu\nu\alpha\beta} \langle \partial_\mu V_\nu \partial_\alpha V_\beta P \rangle. \tag{10}$$

$\mathcal{L}_{VPP}$ appears in the local hidden-gauge approach and $\mathcal{L}_{VVP}$ can be found from [81,82], where G' is given by

$$G' = \frac{3g'}{4\pi^2 f}, \qquad g' = -\frac{G_V m_\rho}{\sqrt{2} f^2},$$
$$G_V = 55 \text{ MeV}, \qquad f = 93 \text{ MeV}.$$

In addition to V^μ of Eq. (2) we now need the matrix P for the pseudoscalar mesons given by

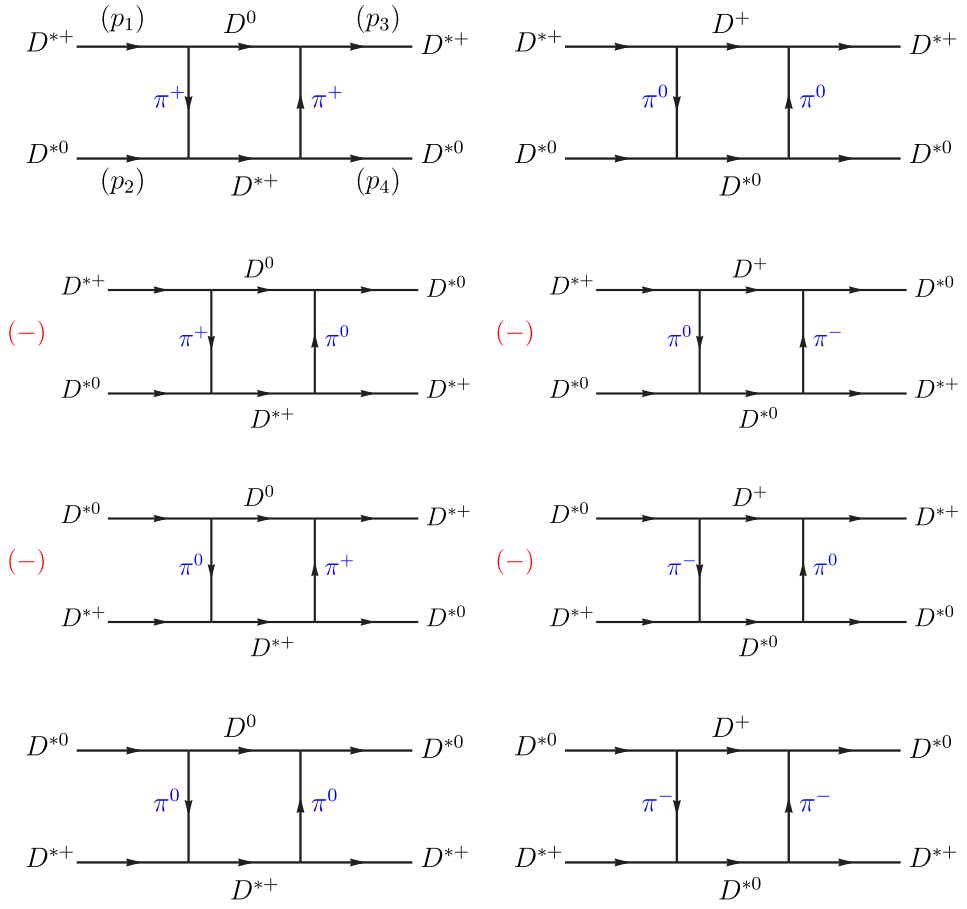

FIG. 3. Box diagrams according for the $D^* D^*, I = 0$ decay into $D^0 D^{*+}$ and $D^+ D^{*0}$.

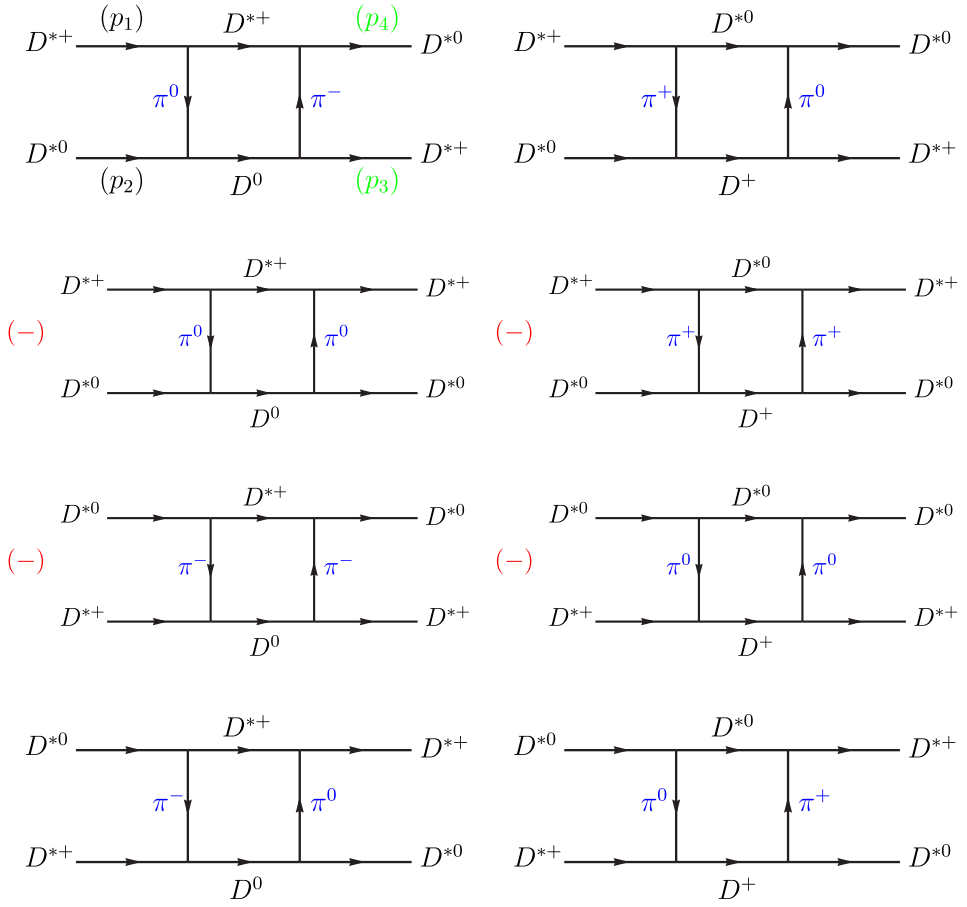

FIG. 4. Diagrams obtained from Fig. 2 exchanges $D^*(p_3) \leftrightarrow D^*(p_4)$ in the final state.

$$P = \begin{pmatrix} \frac{\eta}{\sqrt{3}} + \frac{\eta'}{\sqrt{6}} + \frac{\pi^0}{\sqrt{2}} & \pi^+ & K^+ & \bar{D}^0 \\ \pi^- & \frac{\eta}{\sqrt{3}} + \frac{\eta'}{\sqrt{6}} - \frac{\pi^0}{\sqrt{2}} & K^0 & D^- \\ K^- & \bar{K}^0 & -\frac{\eta}{\sqrt{3}} + \sqrt{\frac{2}{3}}\eta' & D_s^- \\ D^0 & D^+ & D_s^+ & \eta_c \end{pmatrix}, \tag{11}$$

where the standard η, η' mixing of [83] has been used.

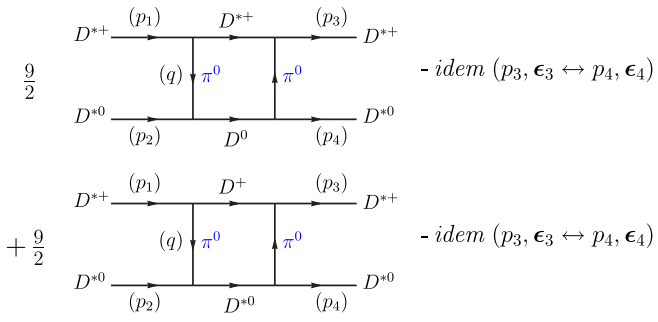

FIG. 5. Diagrams to be calculated with their respective weights.

We evaluate the amplitudes at the D^*D^* threshhold since we expect small binding energies. We have then $\epsilon^0 = 0$ for all the external vector mesons and we take it also for the propagating vectors in the loop given the large mass of the particles. We get the following vertices:

(1) $D^{*0}\pi^0 \to D^0$,
$$-it = -2i\, g\, \boldsymbol{q}\boldsymbol{\epsilon}(D^{*0})\, \tfrac{1}{\sqrt{2}},$$
(2) $D^0 \to \pi^0 D^{*0}$,
$$-it = -2i\, g\, \boldsymbol{q}\boldsymbol{\epsilon}(D^{*0})\, \tfrac{1}{\sqrt{2}},$$
(3) $D^{*+} \to \pi^0 D^{*+}$,
$$-it = -i\, \tfrac{G'}{\sqrt{2}} \epsilon^{ijk} E(D^{*+}_{\rm ext}) \epsilon_i(D^{*+}_{\rm ext}) q_j\, \epsilon_k({\rm int})\, \tfrac{1}{\sqrt{2}},$$
(4) $D^{*+}\pi^0 \to D^{*+}$,
$$-it = -i\, \tfrac{G'}{\sqrt{2}} \epsilon^{ijk} E(D^{*+}_{\rm ext}) \epsilon_i(D^{*+}_{\rm ext}) q_j\, \epsilon_k({\rm int})\, \tfrac{1}{\sqrt{2}},$$

where all vector and tensor components are contravariant (even if we write them as lower indices) and $E(D^*)$ stands for the energy of the D^*. The indices "ext" or "int" stand for the external or internal vectors of the diagrams.

Taking into account that

$$\sum_{\rm pole} \epsilon_k({\rm int}) \epsilon_{k'}({\rm int}) = \delta_{kk'},$$

the product of all four vertices gives

$$(\sqrt{2}g)^2\left(\frac{G'}{2}\right)^2 E(1)E(3)\{\epsilon_i(1)\epsilon_l(2)\epsilon_i(3)\epsilon_m(4)\boldsymbol{q}^2 q_l q_m - \epsilon_j(1)\epsilon_l(2)\epsilon_i(3)\epsilon_m(4)q_i q_j q_l q_m\}, \quad (12)$$

where the indices 1,2,3,4 refer to the particles on the order of Fig. 5. Let us note that at threshold all the propagators in the loop depend only on $\boldsymbol{q}^2$ which allows us to write

$$\int d^3q f(\boldsymbol{q}^2)q_l q_m = \int d^3q f(\boldsymbol{q}^2)\frac{1}{3}\boldsymbol{q}^2\delta_{lm},$$
$$\int d^3q f(\boldsymbol{q}^2)q_i q_j q_l q_m = \int d^3q f(\boldsymbol{q}^2)\frac{1}{15}\boldsymbol{q}^4(\delta_{ij}\delta_{lm} + \delta_{il}\delta_{jm} + \delta_{im}\delta_{jl}). \quad (13)$$

The second combination in Eq. (12) gives rise to the product of polarization vectors in the order of 1,2,3,4

$$\epsilon_j\epsilon_l\epsilon_j\epsilon_l + \epsilon_j\epsilon_i\epsilon_i\epsilon_j + \epsilon_j\epsilon_j\epsilon_i\epsilon_i, \quad (14)$$

and using the projectors into the spin states of $J = 1, 2, 3$, $\mathcal{P}^{(0)}$,$\mathcal{P}^{(1)}$,$\mathcal{P}^{(2)}$ from [40,74] we have

$$\epsilon_j\epsilon_j\epsilon_i\epsilon_i = 3\mathcal{P}^{(0)},$$
$$\epsilon_j\epsilon_l\epsilon_j\epsilon_l = \mathcal{P}^{(0)} + \mathcal{P}^{(1)} + \mathcal{P}^{(2)},$$
$$\epsilon_j\epsilon_i\epsilon_i\epsilon_j = \mathcal{P}^{(0)} - \mathcal{P}^{(1)} + \mathcal{P}^{(2)}. \quad (15)$$

Hence, the combination of Eq. (14) gives

$$\mathcal{P}^{(0)} + \mathcal{P}^{(1)} + \mathcal{P}^{(2)} + \mathcal{P}^{(0)} - \mathcal{P}^{(1)} + \mathcal{P}^{(2)} + 3\mathcal{P}^{(0)},$$

and we see that this term does not contribute to our state with $J^P = 1^+$. The first term of Eq. (12) gives rise to the combination

$$\epsilon_i\epsilon_l\epsilon_i\epsilon_l = \mathcal{P}^{(0)} + \mathcal{P}^{(1)} + \mathcal{P}^{(2)},$$

One can see that the diagrams of Fig. 3 give rise to the same combination, and those of Fig. 5 and the equivalent to Fig. 3 exchanging $p_3, \boldsymbol{\epsilon}_3 \leftrightarrow p_4, \boldsymbol{\epsilon}_4$ give the same contribution except for a minus sign and the exchange of $\boldsymbol{\epsilon}_3 \leftrightarrow \boldsymbol{\epsilon}_4$. Hence we get the combination now of

$$-\epsilon_i\epsilon_l\epsilon_l\epsilon_i = -(\mathcal{P}^{(0)} - \mathcal{P}^{(1)} + \mathcal{P}^{(2)}),$$

and we see that they give the same contribution to $\mathcal{P}^{(1)}$ as the other diagrams. Altogether we find now for the $J^P = 1^+$ state the contribution for the four diagrams of Fig. 5, keeping the positive-energy part of the propagators of the heavy particles

$$-it = 4\frac{9}{2}\frac{1}{3}\int\frac{d^4q}{(2\pi)^4}\frac{1}{2E_{D^*}(\boldsymbol{q})}\frac{i}{p_1^0 - q^0 - E_{D^*}(\boldsymbol{q}) + i\epsilon}\frac{1}{2E_D(\boldsymbol{q})} \times\frac{i}{p_2^0 + q^0 - E_D(\boldsymbol{q}) + i\epsilon}\frac{i}{q^2 - m_\pi^2 + i\epsilon} \times\frac{i}{(p_2 - p_4 + q)^2 - m_\pi^2 + i\epsilon}\boldsymbol{q}^4. \quad (16)$$

The pion propagator cannot be placed on shell and if we are interested in the imaginary part only the D^*D intermediate particles can be put on shell. We can perform the q^0 analytically and then use $\mathrm{Im}\frac{1}{x+i\epsilon} = -i\pi\delta(x)$ (alternatively one can use Cutkowsky rules) and we find

$$\mathrm{Im}V_{\mathrm{box}} = -6\frac{1}{8\pi}\frac{1}{\sqrt{s}}q^5 E_{D^*}^2(\sqrt{2}g)^2\left(\frac{G'}{2}\right)^2 \times\left(\frac{1}{(p_2^0 - E_D(\boldsymbol{q}))^2 - \boldsymbol{q}^2 - m_\pi^2}\right)^2 F^4(q)\,F_{HQ}, \quad (17)$$

where

$$q = \frac{\lambda^{1/2}(s, m_{D^*}^2, m_D^2)}{2\sqrt{s}}, \qquad E_{D^*} = \frac{\sqrt{s}}{2},$$

where we have added the form factor $F(q)$ used in [39,40] and the heavy quark correcting factor F_{HQ} to correct the VPP vertex for heavy particles, as discussed in [84]

$$F(q) = e^{((q^0)^2 - \boldsymbol{q}^2)/\Lambda^2} \quad (18)$$

with

$$q^0 = p_1^0 - E_{D^*}(\boldsymbol{q}),$$

and

$$F_{HQ} = \left(\frac{m_{D^*}}{m_{K^*}}\right)^2$$

2. $D_s^*D^* \to D_s^*D + D_sD^*$ decay

We take the $D_s^{*+}D^{*+}$ state and consider the decay into $D_s^{*+}D^+$ and $D_s^+D^{*+}$. The diagrams that we must consider are now depicted in Fig. 6. Since D_s^* does not couple to $D_s^*\pi^0$ we see that the first and fourth diagrams to the left in Fig. 6 are zero and so are all the diagrams of the right in Fig. 6. We repeat the calculations as done in the former subsection, omitting details and we obtain now

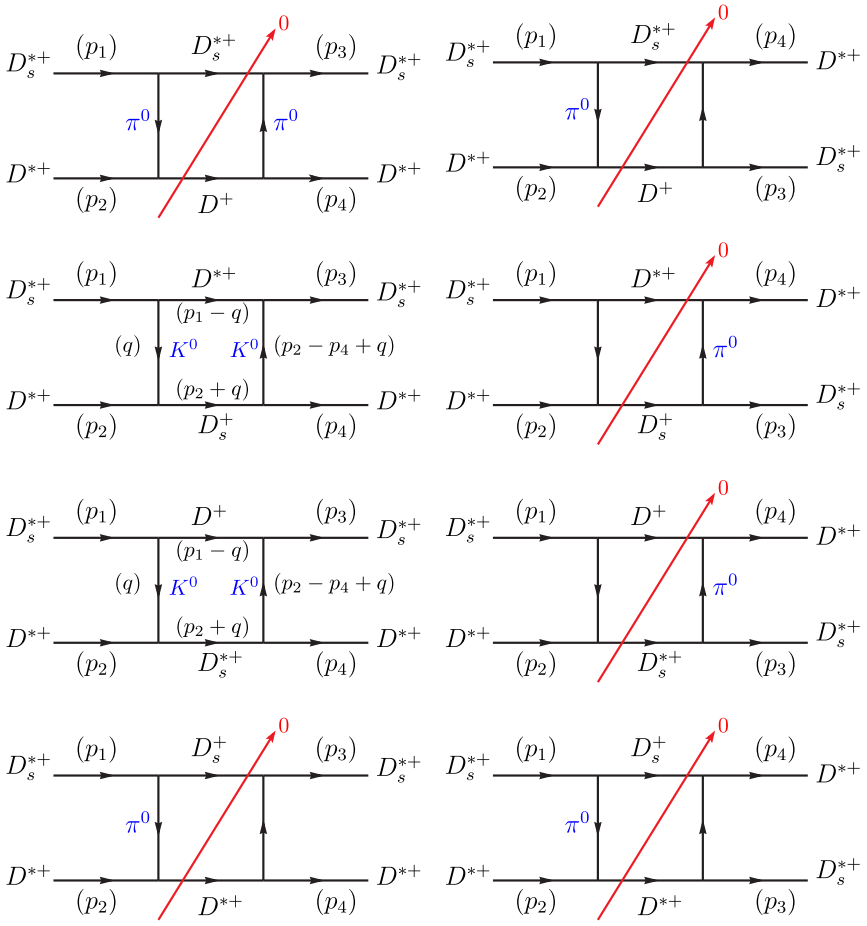

FIG. 6. Diagrams for the decay of $D_s^{*+}D_s^{*+}$ into $D_s^{*+}D^+$ and $D_s^+D^{*+}$.

$$\mathrm{Im}V_{\mathrm{box}} = -\frac{1}{3}\frac{1}{8\pi}\frac{1}{\sqrt{s}}(2g)^2\left(\frac{G'}{\sqrt{2}}\right)^2(E_1E_3+E_2E_4) \times q^5\left(\frac{1}{(p_2^0-E_{D_s}(\boldsymbol{q}))^2-\boldsymbol{q}^2-m_K^2}\right)^2 F^4(q)F_{HQ}, \tag{19}$$

with $F(q)$ given by Eq. (18) with

$$q^0 = p_2^0 - E_{D_s}(\boldsymbol{q}), \qquad q = \frac{\lambda^{1/2}(s, m_{D^*}^2, m_{D_s}^2)}{2\sqrt{s}},$$
$$p_2^0 = \frac{s + m_{D^*}^2 - m_{D_s^*}^2}{2\sqrt{s}}.$$

We then solve the Bethe-Salpeter equation of Eq. (7) with

$$V \to V + i\,\mathrm{Im}V_{\mathrm{box}}$$

for the two cases D^*D^*, $I=0$, $J^P=1^+$ and $D_s^*D^*$, $I=\frac{1}{2}$, $J^P=1^+$ and calculate the T-matrix. By plotting $|T|^2$ we find the mass of the state and its width which we report in the next section.

III. RESULTS

We will use the cutoff method to regularize the loops—something advised in [85]. The value of the cutoff, or subtraction constant in dimensional regularization, is normally the only free parameter in the theory, and this is the case here. One can take reasonable cutoffs from 450 MeV to 750 MeV and make reasonable predictions, but in the present case we can use the cutoff that was needed in [8] to get the experimental binding of the D^*D state and rely upon it. We would then be making use of the findings of [86,87] encouraging the use of the same cutoff to respect rules of heavy quark symmetry, although there are limitations to the use of this symmetry in the case of two heavy quarks as we have here [88–90].

In Fig. 7 we show the results for $|T_{D^*D^*,D^*D^*}|^2$ as a function of $\sqrt{s}$ calculated with a cutoff for G in Eq. (7), $q_{\mathrm{max}} = 750$ MeV, and a value of Λ of Eq. (18) of 1200 MeV, similar to what was used in [39], and also for $\Lambda = 1400$ MeV. We see that the results do not change

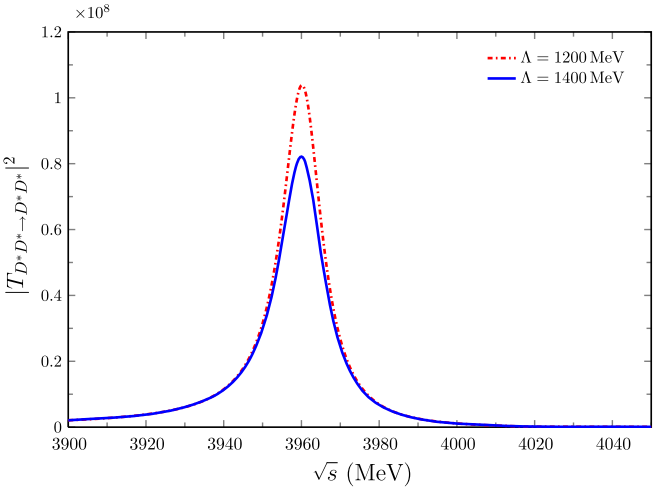

FIG. 7. Squared amplitude $|T_{D^*D^*\to D^*D^*}|^2$ with $q_{\max} = 750$ MeV.

much by changing the value of Λ and we get a bound state around 3960 MeV.

It should be noted that we have two different scales to regularize the different loops. The first one, $q_{\max}$, is used for the loops resulting from the iteration of the diagrams of Fig. 1, where in the t-channel we have the exchange of vector mesons, which are very off shell, to the point that, as usual, we neglect q^2 versus M_V^2, and we obtain the G function for the loop where there are only two propagators. For the diagrams of Figs. 2, 3, 4, we have pion exchange in the t-channel. This pion is light (or kaon in Figs. 6) and we can no longer neglect q^2 versus m_π^2, which forces us to make an exact calculation of the loop with four propagators. The range of q in the integration is also different now. In principle we only know that the scale of the form factors (or cutoffs) is of the order of 1 GeV, but to be more precise we use phenomenological information and take $q_{\max}$ to regularize the G function from the study if the T_{cc} state in [8] and Λ of the form factor to regularize the box diagram from the study of the $D^*\bar{K}^*$ molecule $X_0(2866)$ decaying to $D\bar{K}$, considered in [39,40] with a similar box diagram. Note that since we only evaluate the imaginary part of the box, the effect of the form factor is moderate as shown in Fig. 7.

As we mentioned, the vector mesons exchanged in Fig. 1 (b) are very off shell. They are spacelike (q^2 is negative and small compared to M_V^2) and hence they have no width.[1] Hence, the approximation of $1/(q^2 - M_V^2 + i(q^2)^{1/2}\Gamma(q^2))$ by $1/(-M_V^2)$, as we have done, is a sensible one. We should note that this approximation is the one that produces the chiral Lagrangians from the exchange of vector mesons in the local hidden gauge approach in the $SU(3)$ space [91,92].

In Fig. 8 we show instead the results of $|T_{D^*D^*,D^*D^*}|^2$ for a fixed value of $\Lambda = 1200$ MeV and different values of the cutoff. We can see that there is always a bound state. The binding energy depends on the cutoff value and for values of $q_{\max}$ of the order of 450 MeV, as needed in [8] to get the T_{cc} state, we also obtain a bound state very close to the D^*D^* threshold. We observe a curious phenomena which is that the width becomes smaller as we get closer to the threshold, in spite of the fact that the phase space for decay increases with increasing energy. To understand this feature we recall that including the box diagram in our approach, adding it to the potential from vector exchange and solving the Bethe-Salpeter equation, is an effective way to include the D^*D channel together with D^*D^*, or the D_s^*D, D_sD^* channels together with the $D_s^*D^*$ channel. Then one must recall a well-known fact, based on the Weinberg compositeness condition [93–95], that the coupling squared of the bound state to the hadron-hadron component in a single channel goes as the square root of the binding energy. As we go closer to the D^*D^* threshold the coupling of the resonance to this channel becomes smaller. What is less known is that in the case of coupled channels, if we approach one threshold, all the couplings to the different channels that couple to the one of that threshold also go to zero [95,96]. Then the width of the D^*D^* state obtained will be proportional to the square of the coupling of that state to D^*D and will go to zero as we approach the D^*D^* threshold.

In Fig. 9 we show the results for the $D_s^*D^*$ case. We show the results of $|T_{D_s^*D^*,D_s^*D^*}|^2$ for $q_{\max} = 750$ MeV and two values of the parameter Λ. As we can see, we get a bound state and the width does not change much with the value

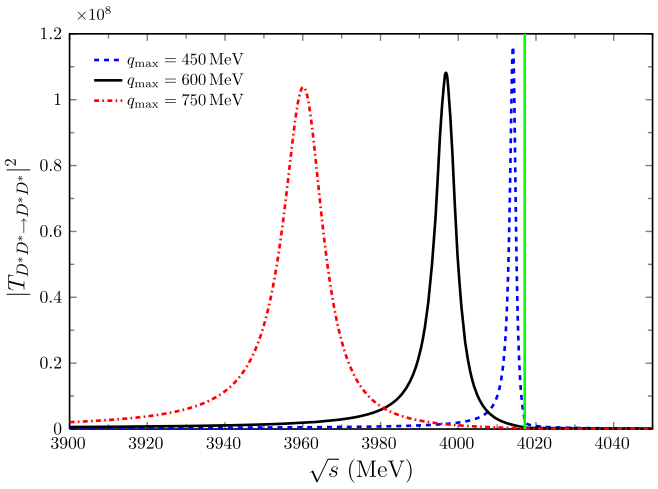

FIG. 8. Squared amplitude $|T_{D^*D^*\to D^*D^*}|^2$ with $\Lambda = 1200$ MeV. The vertical line indicates the D^*D^* threshold at 4017.1 MeV.

[1]One should use a full propagator for the exchanged vector including its width. However, unitarity of the amplitudes requires that the propagator (equivalent to a Breit-Wigner form) is $1/(q^2 - M_V^2 + i(q^2)^{1/2}\Gamma(q^2))$, with the width as a function of q^2, but for $q^2 \le 0$, $\Gamma(q^2) = 0$.

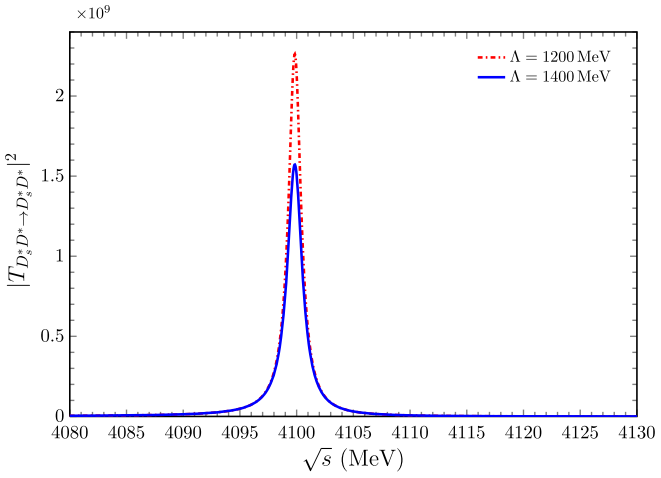

FIG. 9. Squared amplitude $|T_{D_s^*D^*\to D_s^*D^*}|^2$ with $q_{\max} = 750$ MeV.

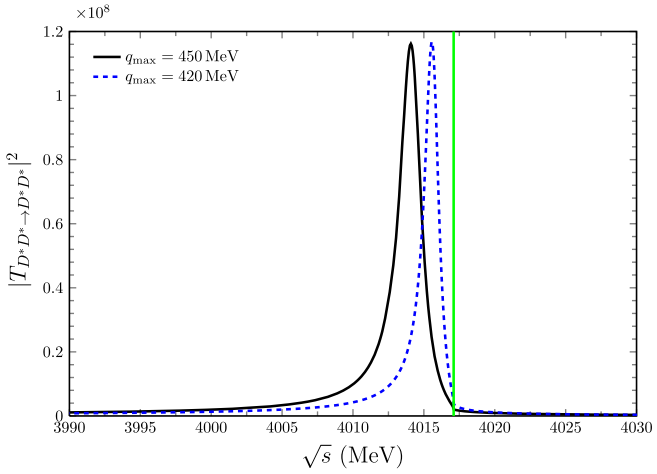

FIG. 11. The same as Fig. 8 but with a smaller range of $q_{\max}$ as in [8].

of Λ. In Fig. 10 we show the results of $|T_{D_s^*D^*,D_s^*D^*}|^2$ for $\Lambda = 1200$ MeV and three values of $q_{\max}$. We see a similar trend as before, but the bindings are smaller as a consequence of the smaller strength of the potential.

In Figs. 11 and 12 we show the enlarged picture of the states in Figs. 8 and 10 for $q_{\max} = 450$ MeV, together with the results for $q_{\max} = 420$ MeV (the value taken in [8] to get the T_{cc} state). For the $D_s^*D^*$ system we do not get bound states in these latter cases, and instead we find pronounced cusps at the $D_s^*D^*$ threshold. This is a consequence of the weaker potential V in the case of $D_s^*D^*$ compared to D^*D^*, Eqs. (4) and (5) (see for instance Tables XVI and XVIII of [39] for numerical values). We summarize this information in Table I, providing the mass and width of the states. Values of the binding around 0.5 MeV–1.5 MeV for the D^*D^* system are also obtained in [30,44] using arguments of heavy quark spin symmetry and the data of [4]. The width is not calculated there. The work of [30] explores the possibility of an $I = 1$ state, not fully ruled out by the data, but our theoretical framework excludes such a state. We think these are sensible predictions that should encourage the search of these states at LHCb.

We can compare the results obtained here with those in Ref. [39] for the D^*D^* and $D_s^*D^*$ systems. Since these systems were investigated theoretically for the first time from the molecular perspective, one could only use a general regulator for the loops which were evaluated with dimensional regularization and a typical subtraction constant was used. Here we have experimental constraints from the mass of the T_{cc} and this allows us to be more precise in the predictions. The masses 4015 MeV and 4122 MeV for D^*D^* and $D_s^*D^*$, respectively, obtained here were found in Ref. [39] as 3969 MeV and 4101 MeV, respectively. Both systems were found as bound systems, but the binding energies were bigger. The small binding found for the T_{cc}

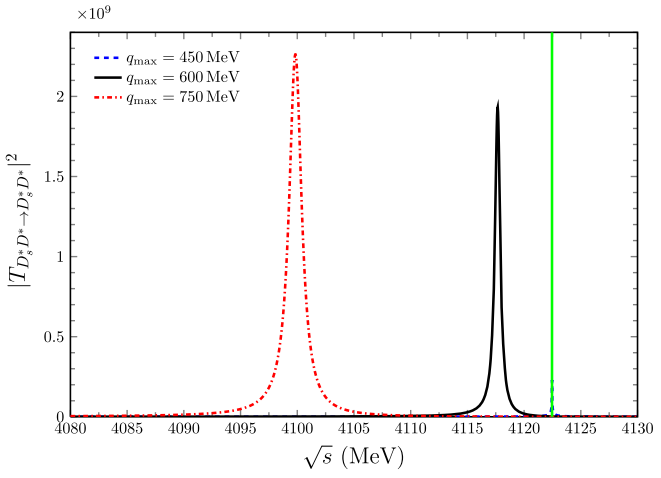

FIG. 10. Squared amplitude $|T_{D_s^*D^*\to D_s^*D^*}|^2$ with $\Lambda = 1200$ MeV. The vertical line indicates the $D_s^*D^*$ threshold at 4122.46 MeV.

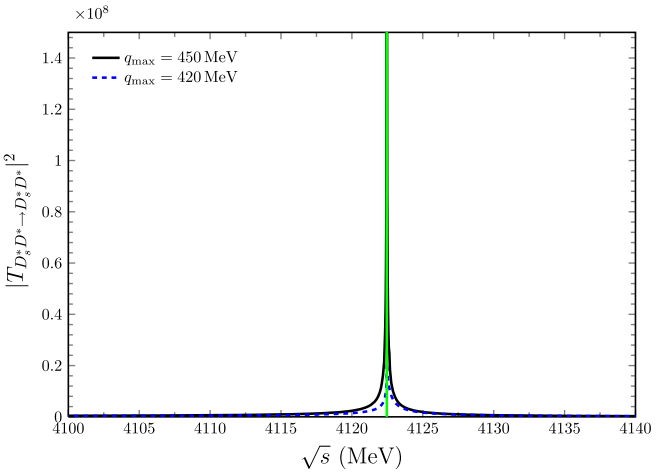

FIG. 12. The same as Fig. 10 but with a smaller range of $q_{\max}$ as in [8].

TABLE I. The predictions assuming the cut off of the order of 420 MeV–450 MeV as in [8]. Threshold mass for D^*D, 4017.1 MeV, and for $D_s^*D^*$, 4122.46 MeV.

	$q_{\max} = 450$ MeV	$q_{\max} = 420$ MeV
$M_{D^*D^*}$	4014.08 MeV	4015.54 MeV
$B_{D^*D^*}$	3.23 MeV	1.56 MeV
$\Gamma_{D^*D^*}$	2.3 MeV	1.5 MeV
$M_{D_s^*D^*}$	4122.46 MeV (cusp)	4122.46 MeV (cusp)
$\Gamma_{D_s^*D^*}$	70–100 KeV	70–100 KeV

state constrains the bindings of these systems to be smaller than found in [39]. In addition, in [39] only the widths of the states decaying to two pseudoscalar mesons were evaluated and, as a consequence, the widths predicted for these states were zero. Here we have explicitly investigated the width of the states decaying to pseudoscalar-vector pairs, driven by an anomalous coupling, and we make predictions for the width of the states.

IV. CONCLUSIONS

Encouraged by the recent experimental observation of the T_{cc} state close to the D^*D threshold, that can be explained as a molecular state of D^*D, we extend the theoretical work on this latter state to the D^*D^* with $I = 0$ and $D_s^*D^*$ with $I = 1/2$ systems, which have been studied in the past and were shown to develop a bound state with $J^P = 1^+$. We also show that these systems with other quantum numbers, or the $D_s^*D_s^*$ system, do not lead to bound states. We have taken advantage of the experimental information on the binding of the T_{cc} state to fix the cutoff regulator of the loops in the Bethe-Salpeter equation. On the other hand, we have included the decay into the D^*D system which involves anomalous couplings, which allows us to get the width of the states—something not done before. The result of our calculations show that both systems give rise to bound states, and assuming the same cut off as was needed in the study of the T_{cc} state, we predict bindings of the order of MeV and also widths of the same order of magnitude for the D^*D^* system, while for the $D_s^*D^*$ system this leads to a pronounced cusp around the threshold with a width of the order of 70 KeV–100 KeV. The width of the D^*D^* system is much larger than the one of the T_{cc} state, 40 KeV–50 KeV, because in this latter case the width is due to the decay of the D^* into $D\pi$ (for which there is very little phase space) but in the present case we have the decay channel D^*D and there is a much larger phase space for the decay. For the $D_s^*D^*$ state the width is much smaller than for the D^*D^* state as a consequence of different factors in the formulas of $\mathrm{Im}V_{\mathrm{box}}$ in Eqs. (17) and (19), and the fact that one has a π exchange in the D^*D^* case while there is a kaon exchange in the case of $D_s^*D^*$. We think the predictions are rather reliable and encourage the LHCb Collaboration to look for these states in the near future.

ACKNOWLEDGMENTS

This work is partly supported by the National Natural Science Foundation of China under Grants No. 11975009, No. 12175066, and No. 12147219. R. M. acknowledges support from the CIDEGENT program with Reference No. CIDEGENT/2019/015 and from the spanish national Grants No. PID2019–106080 GB-C21 and No. PID2020–112777 GB-I00. This work is also partly supported by the Spanish Ministerio de Economia y Competitividad (MINECO) and European FEDER funds under Contracts No. FIS2017-84038-C2-1-P B and No. PID2020–112777 GB-I00, and by Generalitat Valenciana under Contract No. PROMETEO/2020/023. This project has received funding from the European Union Horizon 2020 research and innovation programme under the program H2020-INFRAIA-2018-1, Grant Agreement No. 824093 of the STRONG-2020 project.

[1] F. Muheim, The European Physical Society conference on high energy physics 2021, https://indico.desy.de/event/28202/contributions/102717/.
[2] I. Polyakov, The European Physical Society conference on high energy physics 2021, https://indico.desy.de/event/28202/contributions/105627/.
[3] A. Liupan, https://indico.nucleares.unam.mx/event/1541/session/4/contribution/35/material/slides/0.pdf.
[4] R. Aaij *et al.* (LHCb Collaboration), Phys. Rev. Lett. **125**, 242001 (2020).
[5] N. Li, Z. F. Sun, X. Liu, and S. L. Zhu, Chin. Phys. Lett. **38**, 092001 (2021).
[6] L. Meng, G. J. Wang, B. Wang, and S. L. Zhu, Phys. Rev. D **104**, L051502 (2021).
[7] L. Y. Dai, X. Sun, X. W. Kang, A. P. Szczepaniak, and J. S. Yu, arXiv:2108.06002.
[8] A. Feijoo, W. H. Liang, and E. Oset, Phys. Rev. D **104**, 114015 (2021).
[9] S. S. Agaev, K. Azizi, and H. Sundu, arXiv:2108.00188.
[10] T. W. Wu, Y. W. Pan, M. Z. Liu, S. Q. Luo, X. Liu, and L. S. Geng, arXiv:2108.00923.
[11] X. Z. Ling, M. Z. Liu, L. S. Geng, E. Wang, and J. J. Xie, Phys. Lett. B **826**, 136897 (2022).

[12] R. Chen, Q. Huang, X. Liu, and S.-L. Zhu, Phys. Rev. D **104**, 114042 (2021).
[13] M. J. Yan and M. P. Valderrama, Phys. Rev. D **105**, 014007 (2022).
[14] X. Z. Weng, W. Z. Deng, and S. L. Zhu, Chin. Phys. C **46**, 013102 (2022).
[15] Y. Huang, H. Q. Zhu, L. S. Geng, and R. Wang, Phys. Rev. D **104**, 116008 (2021).
[16] Q. Xin and Z. G. Wang, arXiv:2108.12597.
[17] S. Fleming, R. Hodges, and T. Mehen, Phys. Rev. D **104**, 116010 (2021).
[18] X. Chen, arXiv:2109.02828.
[19] K. Azizi and U.Özdem, arXiv:2109.02390.
[20] H. Ren, F. Wu, and R. Zhu, arXiv:2109.02531.
[21] G. Yang, J. Ping, and J. Segovia, Phys. Rev. D **104**, 094035 (2021).
[22] Y. Jin, S. Y. Li, Y. R. Liu, Q. Qin, Z. G. Si, and F. S. Yu, Phys. Rev. D **104**, 114009 (2021).
[23] Y. Hu, J. Liao, E. Wang, Q. Wang, H. Xing, and H. Zhang, Phys. Rev. D **104**, L111502 (2021).
[24] K. Chen, R. Chen, L. Meng, B. Wang, and S. L. Zhu, arXiv:2109.13057.
[25] J. He, D. Y. Chen, Z. W. Liu, and X. Liu, arXiv:2109.14395.
[26] X. K. Dong, F. K. Guo, and B. S. Zou, arXiv:2108.02673.
[27] L. M. Abreu, F. S. Navarra, and H. P. L. Vieira, arXiv:2110.11145.
[28] Q. Qin, Y. F. Shen, and F. S. Yu, Chin. Phys. C **45**, 103106 (2021).
[29] R. Aaij *et al.* (LHCb Collaboration), arXiv:2109.01056.
[30] M. Albaladejo, arXiv:2110.02944.
[31] M. Bando, T. Kugo, and K. Yamawaki, Phys. Rep. **164**, 217 (1988).
[32] M. Harada and K. Yamawaki, Phys. Rep. **381**, 1 (2003).
[33] U. G. Meissner, Phys. Rep. **161**, 213 (1988).
[34] H. Nagahiro, L. Roca, A. Hosaka, and E. Oset, Phys. Rev. D **79**, 014015 (2009).
[35] J. J. Wu, R. Molina, E. Oset, and B. S. Zou, Phys. Rev. Lett. **105**, 232001 (2010).
[36] N. Isgur and M. B. Wise, Phys. Lett. B **232**, 113 (1989).
[37] M. Neubert, Phys. Rep. **245**, 259 (1994).
[38] A. V. Manohar and M. B. Wise, *Heavy Quark Physics, Cambridge Monographs on Particle Physics, Nuclear Physics and Cosmology* (Cambridge University Press, 2007), Vol. 10.
[39] R. Molina, T. Branz, and E. Oset, Phys. Rev. D **82**, 014010 (2010).
[40] R. Molina and E. Oset, Phys. Lett. B **811**, 135870 (2020).
[41] R. Aaij *et al.* (LHCb Collaboration), Phys. Rev. D **102**, 112003 (2020).
[42] N. Li, Z. F. Sun, X. Liu, and S. L. Zhu, Phys. Rev. D **88**, 114008 (2013).
[43] X. K. Dong, F. K. Guo, and B. S. Zou, Commun. Theor. Phys. **73**, 125201 (2021).
[44] M. L. Du, V. Baru, X. K. Dong, A. Filin, F. K. Guo, C. Hanhart, A. Nefediev, J. Nieves, and Q. Wang, arXiv: 2110.13765.
[45] J. P. Ader, J. M. Richard, and P. Taxil, Phys. Rev. D **25**, 2370 (1982).
[46] S. Zouzou, B. Silvestre-Brac, C. Gignoux, and J. M. Richard, Z. Phys. C **30**, 457 (1986).
[47] L. Heller and J. A. Tjon, Phys. Rev. D **35**, 969 (1987).
[48] J. Carlson, L. Heller, and J. A. Tjon, Phys. Rev. D **37**, 744 (1988).
[49] H. J. Lipkin, Phys. Lett. B **172**, 242 (1986).
[50] Q. Meng, E. Hiyama, A. Hosaka, M. Oka, P. Gubler, K. U. Can, T. Takahashi, and H. S. Zong, Phys. Lett. B **814**, 136095 (2021).
[51] X. Chen, arXiv:2109.02828.
[52] F. S. Navarra, M. Nielsen, and S. H. Lee, Phys. Lett. B **649**, 166 (2007).
[53] M. L. Du, W. Chen, X. L. Chen, and S. L. Zhu, Phys. Rev. D **87**, 014003 (2013).
[54] Z. G. Wang and Z. H. Yan, Eur. Phys. J. C **78**, 19 (2018).
[55] S. S. Agaev, K. Azizi, B. Barsbay, and H. Sundu, Phys. Rev. D **99**, 033002 (2019).
[56] S. S. Agaev, K. Azizi, and H. Sundu, Phys. Rev. D **99**, 114016 (2019).
[57] L. Tang, B. D. Wan, K. Maltman, and C. F. Qiao, Phys. Rev. D **101**, 094032 (2020).
[58] S. S. Agaev, K. Azizi, B. Barsbay, and H. Sundu, Eur. Phys. J. A **57**, 106 (2021).
[59] S. S. Agaev, K. Azizi, B. Barsbay, and H. Sundu, Eur. Phys. J. A **56**, 177 (2020).
[60] S. S. Agaev, K. Azizi, and H. Sundu, arXiv:2108.00188.
[61] K. Azizi and U. Özdem, Phys. Rev. D **104**, 114002 (2021).
[62] Z. S. Brown and K. Orginos, Phys. Rev. D **86**, 114506 (2012).
[63] P. Bicudo and M. Wagner (European Twisted Mass Collaboration), Phys. Rev. D **87**, 114511 (2013).
[64] Y. Ikeda, B. Charron, S. Aoki, T. Doi, T. Hatsuda, T. Inoue, N. Ishii, K. Murano, H. Nemura, and K. Sasaki, Phys. Lett. B **729**, 85 (2014).
[65] P. Bicudo, K. Cichy, A. Peters, B. Wagenbach, and M. Wagner, Phys. Rev. D **92**, 014507 (2015).
[66] A. Francis, R. J. Hudspith, R. Lewis, and K. Maltman, Phys. Rev. Lett. **118**, 142001 (2017).
[67] L. Leskovec, S. Meinel, M. Pflaumer, and M. Wagner, Phys. Rev. D **100**, 014503 (2019).
[68] P. Junnarkar, N. Mathur, and M. Padmanath, Phys. Rev. D **99**, 034507 (2019).
[69] P. Mohanta and S. Basak, Phys. Rev. D **102**, 094516 (2020).
[70] R. J. Hudspith, B. Colquhoun, A. Francis, R. Lewis, and K. Maltman, Phys. Rev. D **102**, 114506 (2020).
[71] A. Ali, A. Y. Parkhomenko, Q. Qin, and W. Wang, Phys. Lett. B **782**, 412 (2018).
[72] A. Ali, Q. Qin, and W. Wang, Phys. Lett. B **785**, 605 (2018).
[73] Q. Qin, Y. F. Shen, and F. S. Yu, Chin. Phys. C **45**, 103106 (2021).
[74] R. Molina, D. Nicmorus, and E. Oset, Phys. Rev. D **78**, 114018 (2008).
[75] L. S. Geng and E. Oset, Phys. Rev. D **79**, 074009 (2009).
[76] J. J. Wu, R. Molina, E. Oset, and B. S. Zou, Phys. Rev. C **84**, 015202 (2011).
[77] R. Aaij *et al.* (LHCb Collaboration), Phys. Rev. Lett. **115**, 072001 (2015).
[78] R. Aaij *et al.* (LHCb Collaboration), Phys. Rev. Lett. **122**, 222001 (2019).
[79] R. Aaij *et al.* (LHCb Collaboration), Sci. Bull. **66**, 1278 (2021).

[80] L. Roca, E. Oset, and J. Singh, Phys. Rev. D **72**, 014002 (2005).
[81] A. Bramon, A. Grau, and G. Pancheri, Phys. Lett. B **344**, 240 (1995).
[82] E. Oset, J. R. Pelaez, and L. Roca, Phys. Rev. D **67**, 073013 (2003).
[83] A. Bramon, A. Grau, and G. Pancheri, Phys. Lett. B **283**, 416 (1992).
[84] W. H. Liang, C. W. Xiao, and E. Oset, Phys. Rev. D **89**, 054023 (2014).
[85] J. J. Wu, L. Zhao, and B. S. Zou, Phys. Lett. B **709**, 70 (2012).
[86] M. Altenbuchinger, L. S. Geng, and W. Weise, Phys. Rev. D **89**, 014026 (2014).
[87] J. X. Lu, Y. Zhou, H. X. Chen, J. J. Xie, and L. S. Geng, Phys. Rev. D **92**, 014036 (2015).
[88] E. E. Jenkins, M. E. Luke, A. V. Manohar, and M. J. Savage, Nucl. Phys. **B390**, 463 (1993).
[89] M. Albaladejo, F. K. Guo, C. Hidalgo-Duque, J. Nieves, and M. P. Valderrama, Eur. Phys. J. C **75**, 547 (2015).
[90] V. Baru, E. Epelbaum, J. Gegelia, C. Hanhart, U. G. Meißner, and A. V. Nefediev, Eur. Phys. J. C **79**, 46 (2019).
[91] G. Ecker, J. Gasser, H. Leutwyler, A. Pich, and E. De Rafael, Phys. Lett. B **223**, 425 (1989).
[92] J. M. Dias, G. Toledo, L. Roca, and E. Oset, Phys. Rev. D **103**, 116019 (2021).
[93] S. Weinberg, Phys. Rev. **130**, 776 (1963).
[94] V. Baru, J. Haidenbauer, C. Hanhart, Yu. Kalashnikova, and A. E. Kudryavtsev, Phys. Lett. B **586**, 53 (2004).
[95] D. Gamermann, J. Nieves, E. Oset, and E. Ruiz Arriola, Phys. Rev. D **81**, 014029 (2010).
[96] H. Toki, C. Garcia-Recio, and J. Nieves, Phys. Rev. D **77**, 034001 (2008).